2024 IEEE International Conference on Robotics and Automation (ICRA 2024)
May 13-17, 2024. Yokohama, Japan

Short term after-effects of small force fields applied by an upper-limb exoskeleton on inter-joint coordination

Océane Dubois[1*], Agnès Roby-Brami[1], Ross Parry[2], Nathanaël Jarrassé[1]

Abstract— **Exoskeleton technologies have numerous potential applications, ranging from improving human motor skills to aiding individuals in their daily activities. While exoskeletons are increasingly viewed, for example, as promising tools in industrial ergonomics, the effect of using them on human motor control, particularly on inter-joint coordination, remains relatively uncharted. This paper investigates the effects of generic low-amplitude force fields applied by an exoskeleton on motor strategies in asymptomatic users. The force fields mimic common perturbations encountered in exoskeletons, such as residual friction, over/under-tuned assistance, or structural elasticity. Fifty-five participants performed reaching tasks while connected to an arm exoskeleton, experiencing one of five tested force fields. Their movements before and after exposure to the exoskeleton force field were compared. The study focuses both on spatial and temporal changes in coordination using specific metrics. The results reveal that even brief exposure to a low-amplitude force field, or to uncompensated residual friction and dynamic forces, applied at the joint level can alter the inter-joint coordination, while task performance remains unaffected. The tested force fields induced varying degrees of changes in joint contributions and synchronization. This study highlights the importance of monitoring coordination changes to fully understand the impact of exoskeletons on human motor control and thus enable safe and widespread adoption of those devices.**

I. Introduction

Exoskeletons represent a groundbreaking technological advancement with the potential to significantly enhance human capabilities and aid individuals in their daily activities. These wearable devices serve a multifaceted purpose, including augmenting existing abilities, compensating for lost functions, and preserving motor capabilities. Since 2010, there have been numerous advancements in the field of industrial ergonomics, resulting in the availability of several commercially accessible simple joint exoskeletons. These exoskeletons assist industrial workers in reducing stress and fatigue while carrying loads or maintaining specific postures for extended periods [1] [2] [3].

However, it's important to recognize that while exoskeletons are designed to benefit users, their usage can disrupt motor control due to the close physical interaction with the body. Prolonged use in industrial settings may worsen these effects. Prior studies have extensively analyzed perturbation force fields at the end-effector level using manipulandum robots, which involve a single port of perturbation [4]. In contrast, research on the impact of exoskeletons, which interact at the joint level through multiple ports, has been relatively scarce.

Some studies have examined adaptation to exoskeleton-applied force fields on single joints, revealing altered joint trajectories while maintaining unchanged hand trajectories [5]. Recent research has shown increasing interest in understanding the impact of exoskeletons on the human body, including studies on the evolution of joint coordination post-exposure to force fields [6] or the impact of passive exoskeletons on whole-body joint torques [7]. However, the impact of exoskeletons on human inter-joint coordination remains relatively unexplored due to its complex nature, involving both spatial and temporal aspects of joint movements [8] [9] [10].

This study aims to examine how generic force fields from exoskeletons affect inter-joint coordination in asymptomatic users. The force fields replicate common perturbations found in both active and passive exoskeletons, including residual friction, over/under-tuned assistance, or approximate compensation mechanisms [11].

In our study, 55 participants were asked to perform reaching tasks while connected to a 4 Degree of Freedom (DoF) arm exoskeleton applying one weak magnitude force field (among 4 different tested fields). Their movements both before and after exposure to the exoskeleton force field were recorded using an optical motion capture system. Movements before and after exposure to this perturbation were then analyzed for comparison. To assess the temporal and spatial changes in their coordination strategy, specific metrics were used, including Joint Contribution based on Principal Component Analysis (JcPCA) and Joint Synchronization based on Continuous Relative Phase (JsCRP). The rest of the paper is organized as follows. We first present the experimental protocol and setup that was used, including the two metrics used to assess the inter-joint coordination (Section II). Experimental results are then provided (Section III) and discussed (section IV).

II. Material & Method

A. Exoskeleton

The force fields are generated by a highly backdrivable 4-DoF exoskeleton, ABLE from the CEA-List, designed for the right arm. This exoskeleton has 3-DoF at the shoulder (for abduction/adduction θ_1, internal/external rotation θ_2, and flexion/extension θ_3) and one at the elbow (for flexion/extension θ_4), as shown in Fig. 1. Its mechanical design ensures high efficiency and low residual friction torques,

* Correspondance : dubois@isir.upmc.fr
[1]Sorbonne Universités, CNRS, UMR 7222, INSERM, the Institute of Intelligent Systems and Robotics (ISIR), 4 place Jussieu, 75005 Paris, France
[2]LINP2, Université Paris-Nanterre, 200 avenue de la République, 92001 Nanterre Cedex

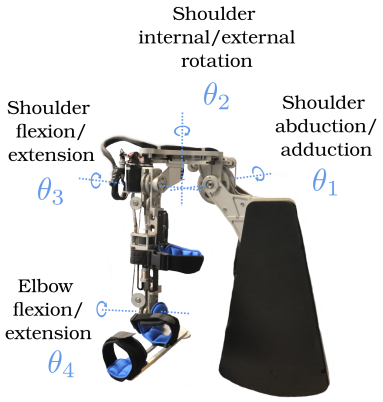

(a) ABLE 4 DoF exoskeleton

Joints	θ_1	θ_2	θ_3	θ_4
Dry Friction (Nm)	0.2	0.15	0.19	0.7
Viscous Friction ($mNm.rad^{-1}.s^{-1}$)	1.31	0.86	0.27	0.6

(b) Experimentally identified residual joint friction of Able exoskeleton

Fig. 1: Exoskeleton design and joint friction

thanks to patented actuators [12] (details in Table of Fig. 1b). In the current study, θ_1 and θ_2 were blocked in position, only θ_3 and θ_4 were used.

B. Exoskeleton's controller

Control algorithms are implemented on a real-time controller (RTLinux) with a control loop running at 1 kHz. The default control mode is Gravity Compensation, which allows unrestricted upper-limb motion. This mode involves a feedforward gravity compensation based on a quasi-static model of the exoskeleton. While this mode minimizes resistance to the user's movements [13], it does exhibit some undesired resistance due to the absence of friction and dynamic compensation. This mode will be known as the *Transparent* condition of the experiment.

Four other control modes have been designed which can be added to the always-on "transparent" reference condition, to reproduce the typical perturbing force fields on the two joints θ_3 and θ_4 : *elastic*, *viscous*, *increased* and *decreased gravity*. The values of the force fields parameters were chosen experimentally to apply a limited perturbation while remaining perceptible by users.

Viscous: In exoskeletons a viscous field can appear at the joint level because of uncompensated friction created in the transmissions. In this experiment, friction is generated on each joint, depending on each joint's velocity such as $\tau = K_v\dot{\theta}$. Where τ is the vector of the output torque of the exoskeleton joints θ_3 and θ_4 sent as a feedforward with $\tau = [\tau_3\,, \tau_4]$ and K_v a vector containing friction coefficients for each joint such as $K_v^T = [2,\ 0.6]$.

Elastic: An elastic field can be generated in exoskeletons by some mechanical elasticity of the structure or by the wrongly adjusted equilibrium point of a spring mechanism.

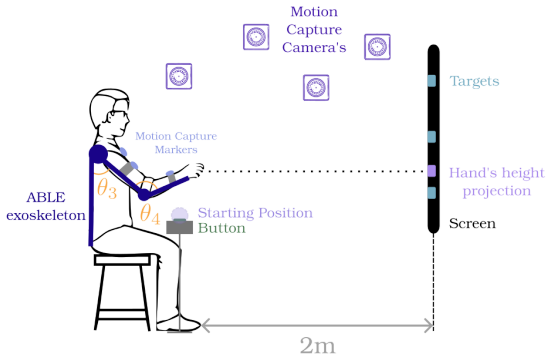

Fig. 2: Experimental Set-up

Here, a reference position is defined as θ_0 and the elastic mode is defined as $\tau = K_e(\theta_i - \theta_{i,0})$ where τ is the vector of the output torque of the exoskeleton joints θ_3 and θ_4 sent as a feedforward as $\tau = [\tau_3\,, \tau_4]$ and K_e a vector containing stiffness values for each joint such as $K_e^T = [3.5\,, 2]$.

Decreased Gravity: Decreased gravity fields are encountered in poorly adjusted passive industrial exoskeletons, causing overcompensation of limb and/or tool weight, making the user's arm feel lighter. Here, decreased gravity mode corresponds to the over-compensation of 25% of the exoskeleton mobile part weight, hence the user feels as if their arm is 750 grams lighter. In the controller, this is done by simply modulating the gravity vector by 0.75 of the feedforward gravity compensation.

Increased Gravity : Similarly such field can be met on badly adjusted exoskeleton giving the user the impression that his arm is heavier. Increased gravity mode corresponds to the under-compensation of the exoskeleton mobile parts weight by 25% (+750 grams). Again, here, this is done by modulating the gravity vector by 1.25 of the feedforward gravity compensation.

C. Motion Capture System and Data Recording

A motion capture system (OptiTrack, NaturalPoint, USA) tracks participant movements using markers placed on their trunk, arm, forearm, and hand. Markers do not need to be placed at specific locations as the calibration algorithm (see II-G) doesn't demand specific placements. Four cameras positioned around the participant capture movements comprehensively, recording data at 120Hz.

D. Task and Set-up

The experiment has been designed to be redundant as well as being a simple minimal case of study. It consists in a pointing task involving one DoF controlled by two DoF of the upper-limb. Precisely, the height of the extremity of the exoskeleton (figuring the hand of the user) is used to control the height of a bird-shaped cursor presented on a screen placed 2 meters in front of the participant, as well as the targets to reach (Fig. 2). During the experiment, the participant is seated on a stool and instructed to lean against the back structure of the exoskeleton. A button is placed next to him so that his hand naturally rest on the

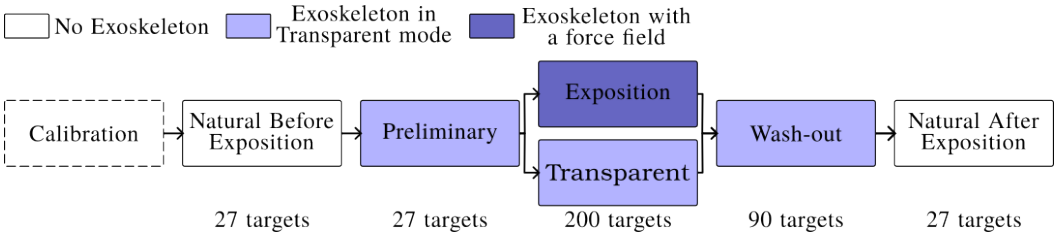

Fig. 3: Experimental protocol

button in a comfortable arm position with the elbow slightly bent, around 130°. The button defines a repeatable starting position for the hand. For each trial, a target, represented as a horizontal line on the screen, is presented at one out of nine heights, in random order. The instruction is to reach the target using two DoFs of the exoskeleton: shoulder (θ_3) and elbow flexion/extension (θ_4). The other two exoskeleton DoFs are blocked, restricting the hand movement to a vertical parasagittal plane aligned with the participant's shoulder. The wrist is immobilized using a pre-made orthosis. Thanks to redundancy, the target can be reached by an infinite number of hand positions along an anteroposterior line at the height of the target in the sagittal plane. In the natural condition, reaching without the exoskeleton (but with the trunk blocked and wrist orthesis) the redundancy involves 4 DoF (3 Shoulder DoF and elbow flexion/extension).

E. Protocol

The experimental protocol consists of six distinct phases (Fig. 3). During the *Calibration* phase, the participant performs random, slow, and large movements without the exoskeleton for one minute. The *Natural Before Exposition* as well as the *Natural After Exposition*, occurs without the exoskeleton. Here, the participant encounters 27 targets (each of the 9 targets presented 3 times in random order). They press the button to initiate the reaching task, the target appears on the screen and the participant then reaches for it naturally, utilizing their arm's 4 DoF. Once the hand remains steady at the target height for 2 seconds, the target is confirmed, and the participant can proceed to the next target by pressing the button. In the *Preliminary* as well as the *Washout* phase, participants wear the exoskeleton in *Transparent* mode, and the first two joints are blocked. They encounter respectively 27 targets (3 times each target) and 90 targets (10 times each target) presented randomly and follow the same reaching procedure. In the *Exposition* phase, participants wear the exoskeleton with the first two joints blocked and experience one force field while reaching 200 targets (40 times for each of the 5 exposed targets). Each participant is exposed to a unique force field among the 4 to prevent any interference between different force field impacts. One group is exposed only to the Transparent force field. They can take breaks as desired. The exposure lasts 15 to 25 minutes.

F. Participants

11 participants were exposed to each force field and 11 to the transparent mode only. For a total of 55 participants with the mean height and age being the same for the 5 groups and the same number of men and women as well as left and right-handed people participated in each group. Each subject filled the Edinburgh inventory [14] to rate their level of left or right-handedness. Left and right-handed people were then balanced between groups.

The study was approved by the local ethics committee at Sorbonne University, and the participants provided informed consent prior to their participation in this study.

G. Data Analysis

Sensors' raw position and orientation are used to identify the participant's joint rotation centers using a calibration algorithm [15]. This algorithm provides the position of each joint rotation center (shoulder and elbow). Data are filtered using a low-pass filter with a 5Hz cutoff frequency. From the shoulder and elbow position, the joint's angle are extracted. Here, the joints' angles are extracted using the exoskeleton joint angle sequence: θ_1, θ_2, θ_3 and θ_4 (see Fig. 1). Movements are then separated into single movement. A movement starts with the button press and ends with the target validation.

For each phase of the protocol, end-effector and joint metrics are computed: task time, overshoot (i.e, the distance between the end-effector maximum height and the target height), distance covered by the end-effector, maximum end-effector velocity, time taken to reach the maximum end-effector velocity, and individual joints range of motion (ROM). Additionally, 2 different metrics are used to assess spatial or temporal changes of inter-joint coordination: Joint contribution with Principal Component Analysis (JcPCA) for the spatial aspect of inter-joint coordination, and Joint synchronization with Continuous Relative Phase (JsCRP) for the temporal aspect of inter-joint coordination.

1) Joint Contribution based on PCA (JcPCA): To reduce the dataset dimensionality, PCA is commonly used [16]. However, it's challenging to interpret inter-joint coordination from PCA analysis [17] [18]. Fig. 4 outlines the method employed to compare PCA outcomes from two sets of joint positions (before and after exposure). To facilitate comparison, data are projected into the reference frame defined by PCA performed on the initial dataset. This allows for a comparison solely based on coefficient weights, disregarding variance percentages. Absolute weight coefficients are utilized for simplicity. A negative JcPCA result indicates reduced joint usage in the second dataset compared to the first, while a positive result signifies increased joint usage.

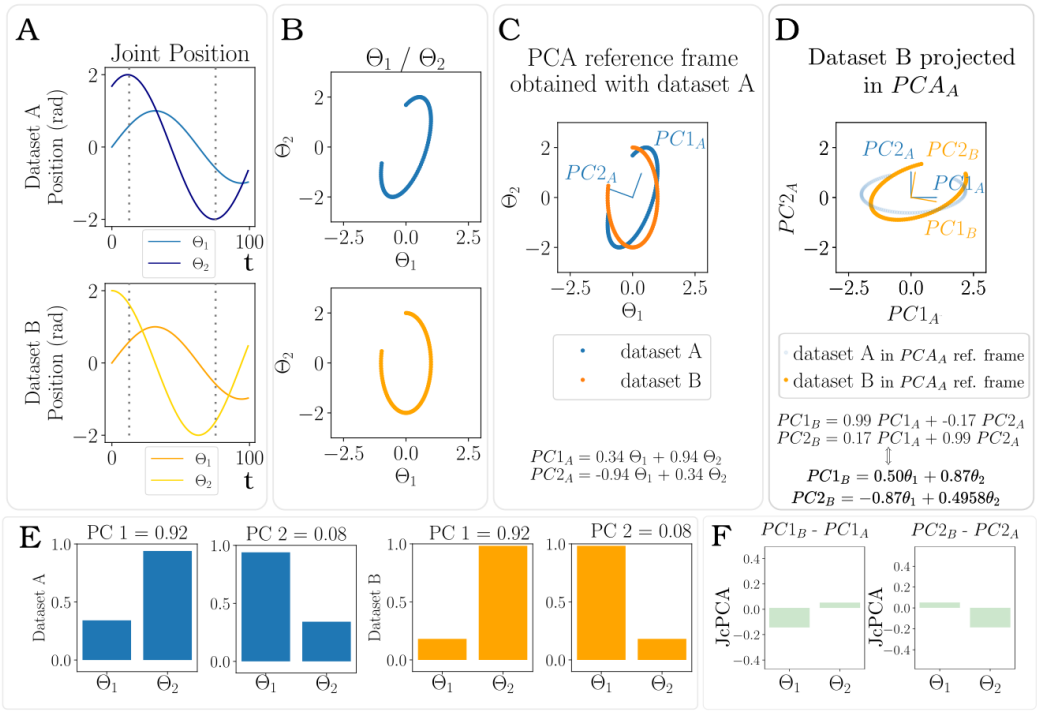

Fig. 4: JcPCA on example data. A: 2 datasets containing joint position. B: Plots of the dataset variables together. C: PCA is computed on the first centered dataset. D: Data of the second dataset are centered and projected in the reference frame defined by the first PCs of the first dataset. Another PCA is conducted on the projected data. E: The coefficients for each joint are extracted from equations on C and D and represented as bar plots for each dataset. F: Each weight coefficient of the datasets is subtracted to show the evolution of the joint contribution between datasets.

In this study, focusing on two joints, this metric aids in determining variations in joint contribution within the task space (first PC) and null space (second PC).

2) Joint Spatio-temporal synchronization based on CRP (JsCRP): Continuous Relative Phase (CRP)is a metric that extracts the phase angle between joint's position and velocity and compare the joint's phases together [19] [20] [21] [22] [23]. In this study, the area between 2 CRP curves is defined as JsCRP and used to quantify the dissimilarities between the 2 curves (Fig. 5). A large area highlights a substantial change in coordination strategy between datasets. Analyzing significant differences between these curves in various regions helps identify when specific moments display the most distinct coordination strategies.

3) Metrics variability: To differentiate between inherent participant variation and true coordination changes, JsCRP and JcPCA are repeatedly calculated using sub-datasets from the Natural Before Exposition condition. This baseline reflects participants' natural variability. When analyzing the *Natural After Exposition* dataset, exceeding the baseline value plus the group's standard error indicates a significant coordination strategy shift.

III. Results

A. Group Homogeneity

Groups' homogeneity in the *Natural Before Exposition* condition was tested across all end-effector metrics and joint range of motion. No statistical differences were found between the groups before exposure to the exoskeleton.

B. End-effector and joints results

Mean and standard deviation by subjects and then by condition are computed on the relative difference between *Before* and *After exposition* condition for each end-effector metric and joint's range of motions. Results are presented in Table I. Statistical tests are then performed on the relative difference of the end-effector and joints metrics in order to test if the different force fields impact differently the joint and end-effector metrics. Kruskal-Wallis test is used as none of the data follow a normal distribution and results are shown in Table II. This first analysis enhances that there is no significant difference between force field conditions for most of the metrics. Dunn's post-hoc test is used to analyze metrics results for which the p-value is lower than 0.05. Both for the overshoot metric and the ROM of θ_3 shoulder flexion/extension), the exposition to viscous force field lead to significant differences. The effect of laterality has also been tested; there are no statistical differences between the left and right-handed people.

C. Inter-joint coordination results

Only results from joints exposed to different force fields (θ_3 and θ_4) are presented here. Table III displays, for each force field and coordination change metric, the number of

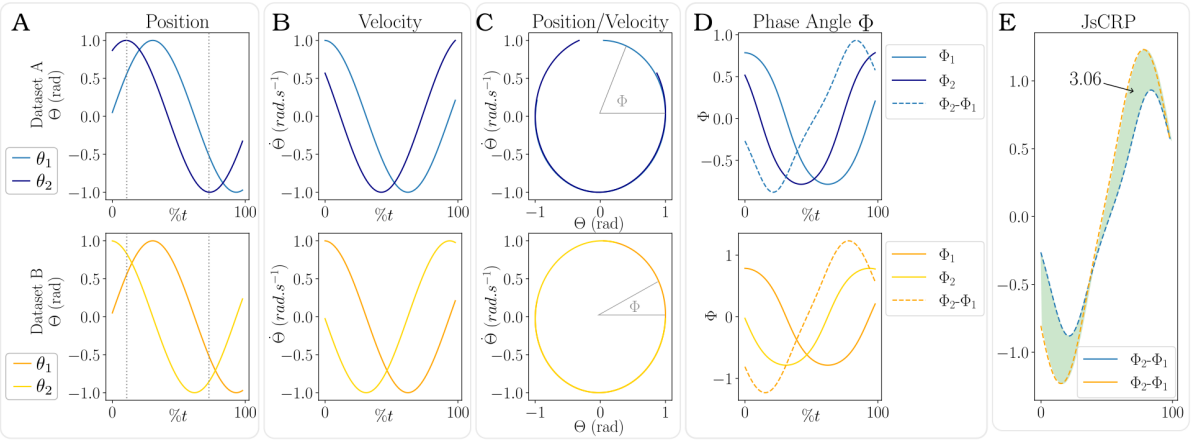

Fig. 5: JsCRP on example data. A 2 dataset composed of joints position. B: range normalized joints' velocities. C: positions and velocities are plotted together. D: the phase angle, which is the angle between each point in time and the horizontal axis is extracted. E: The CRP is calculated as the difference between the phase angles of two joints and the area between the 2 curves is computed.

	End-effec. distance (%)	Overshoot (%)	Maximum End-effec. velocity (%)	Task Time (%)	Time to maximum velocity (%)
Transp.	-0.1±0.16	-0.97±2.48	0.00±0.34	-0.05±0.23	-0.03±0.33
Elastic	-0.04±0.17	-0.20±0.74	0.10±0.46	-0.06±0.33	-0.06±0.28
Viscous	0.07±0.17	0.5±0.4	0.01±0.51	-0.13±0.22	-0.16±0.35
Decr.	-0.15±0.18	-0.63±1.35	-0.17±0.63	-0.08±0.24	0.03±0.23
Incr.	-0.04±0.18	-0.23±1.47	-0.65±2.32	-0.01±0.18	0.06±0.18

(a) End-effector metrics

	ROM θ_1 (%)	ROM θ_2 (%)	ROM θ_3 (%)	ROM θ_4 (%)
Transp.	-0.39±0.87	-0.03±0.13	-0.20±0.55	0.08±0.31
Elastic	-0.48±0.95	-0.02±0.21	0.15±0.23	-0.05±0.38
Viscous	0.09±0.37	-0.18±0.33	0.40±0.27	-0.45±0.57
Decr.	-0.57±0.81	-0.05±0.31	-0.18±0.44	0.00±0.36
Incr.	-1.28±2.11	-0.06±0.47	0.10±0.56	-0.18±0.75

(b) Joints metrics

TABLE I: Mean and standard deviation of the difference between the *Natural Before Exposition* and *Natural After Exposition* condition on the end-effector and joints metrics

	Metric	Factor	Statistic	df	p
End effector metrics	End-effector distance	Field	7.568	4	0.109
	Overshoot	Field	9.639	4	0.047
	Maximum Velocity	Field	0.794	4	0.939
	Task-time	Field	1.803	4	0.772
	Time to Max. Vel.	Field	2.863	4	0.581
Joints metrics	ROM θ_1	Field	6.523	4	0.163
	ROM θ_2	Field	1.111	4	0.892
	ROM θ_3	Field	16.305	4	0.003
	ROM θ_4	Field	5.571	4	0.234

TABLE II: Kruskal-Wallis Test on end-effector metrics and joints metrics

	Transp.	Elastic	Viscous	Decr.	Incr.
JcPCA θ_3	8	7	10	11	8
JcPCA θ_4	6	8	9	6	9
JsCRP θ_3/θ_4	7	7	4	7	9

TABLE III: Number of participants (out of 11 per group) that responded to each force field

participants whose coordination was modified after exoskeleton exposure. This table indicates the count of subjects whose inter-joint coordination metric results exceeded baseline, representing normal variability. Several observations stand out. Firstly, the *Viscous* and *Decreased Gravity* conditions had the most significant impact on joint contribution (JcPCA). Interestingly, even the *Transparent* condition affected over half of the participants' coordination. Additionally, more participants changed their θ_3 contribution than θ_4 movement. While inter-joint synchronization (JsCRP) was less affected overall, over half of the participants were impacted by the *Elastic* force field. The *Viscous* condition had the least impact on inter-joint synchronizations.

The 2 first plots of Fig. 6 present the box plots of the absolute magnitude of the deviation of JcPCA from the baseline for all participants. The baseline is represented in yellow. The *Viscous* and *Increased gravity* force fields are the one that changes the most the joints' contributions. The changes are more important on θ_3 (shoulder joint). The last plot of Fig. 6 presents the box plot of the magnitude of the deviation of the JsCRP from the baseline for all participants. The baseline variability is presented in yellow. Major changes of joint synchronization are observed for the *Elastic* and the *Increased Gravity* force fields.

IV. Discussion and Limitations

The study found that short exposure ($<$ 25 minutes) to low-amplitude force fields resembling typical exoskeleton defects significantly altered participants' inter-joint coordination, while end-effector performance and individual joint metrics remained unaffected. The *Viscous* force field had the greatest impact on the joint contribution, while *Increased Gravity* induced the most changes in both joint contribution and synchronization. *Elastic* force field primarily affected joint synchronization. Notably, even brief exposure to the

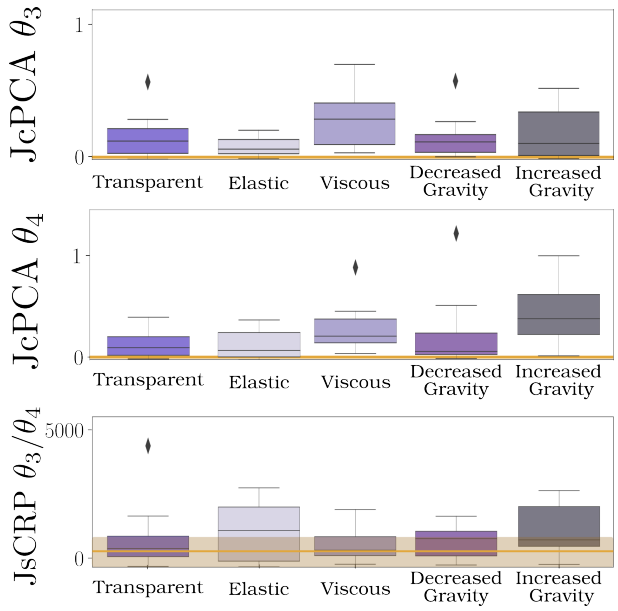

Fig. 6: Inter-joint coordination metrics deviation from the mean behavior for each field. In yellow is represented the baseline variability.

Transparent mode of the exoskeleton resulted in coordination strategy modifications for over half of the participants. This suggests that even short exposures to uncompensated residual (and possibly heterogeneous) joint friction torques can induce changes in participants' coordination strategies.

However, this present study suffers from certain limitations. Firstly, 2 of the 4 DoFs exoskeletons were blocked during the force field exposition. This actually introduces a second force field (rigid blockage) on the two first joints, making it impossible to isolate any potential crossover effect between the force fields on the first two and last two joints. Consequently, the results regarding the first two joints were not presented here, as they could have been influenced by this rigid force field.

In the presented results, the contribution of joint θ_3 was the most affected compared to joint θ_4. This difference could be influenced by the mechanical characteristics of the exoskeleton. For example, the presence of increased friction in the mechanical transmission of the elbow flexion joint θ_4 (see Table 1b) might have reduced the impact of the added force field on this joint, as that intrinsic friction resistive torques were not compensated by the controller. Moreover, since the segments' length of our exoskeleton are not adjustable, the center of rotation of the participant's joint could not be exactly aligned with the exoskeleton's one, creating unwanted residual forces [24] [25] that might influence user's behavior. Most of the time, the participants had their shoulder aligned, creating less residual forces on the shoulder but increasing the potential uncontrolled torques over the elbow joint.

In this study, 55 participants were exposed to 5 different force fields, each requiring varying levels of muscular effort to perform the associated tasks. This implies that some force fields induced more fatigue than others. Unfortunately, the level of fatigue generated by each force field was not quantified in this study, and understanding this aspect could be helpful in correlating the participants' reactions to the force fields [26] [27]. For example, the trunk compensation movements have not been evaluated here, as suggested in [28], taking into account these movements could be a first step to evaluate the muscular fatigue and the compensations induced by the force fields.

Finally, even though the results are enhancing differences in participants' adaptation to the force fields, there are no statistical significant differences in the magnitude of the change of inter-joint coordination between groups. This is due to the large inter-participant variability. Different patterns of inter-joint coordination adaptation have already been enhanced in [6] showing that each subject has its own way of adapting to a perturbation. This effect could be relativized by having a larger number of people taking part in the experiment, in order to extract clearer trends in participants' adaptation.

V. Conclusion and Perspective

This study aims at characterising the after-effects of generic low amplitude perturbing joint force fields applied by an exoskeleton during a short exposition (less than 30 minutes) over the motor strategy of participants. The force fields have been set deliberately small to simulate typical adjustment and compensation faults that can be found in upper-limb exoskeletons, whether they are active or passive (spring-based). Two specific metrics have been used to quantify their effect on both spatial and temporal aspects of inter-joint coordination. The results show that even a brief exposure to a weak force field applied at the joint level can alter joint coordination once the perturbation created by the exoskeleton is removed, even though task performance remains unchanged. Some of the tested force fields create a greater change in the joint's contribution, while others create a greater change in the joint's synchronization. Additionally, the perturbing forces generated by the absence of friction (which is particularly limited on ABLE) or dynamic compensation on the exoskeleton seem sufficient to induce modifications of the participants' coordination strategies.

Currently, the impact of exoskeletons on humans has primarily been studied from an end-effector perspective. However, the results presented here show that even if the end-effector or individual joint performance remains unchanged, the coordination strategies almost always change. This finding highlights that monitoring the coordination changes is crucial to really characterize the impact of exoskeletons on human motor control. Future studies should focus on longer and repeated exposure to the exoskeleton in order to understand short and long-term effects on motor control of wearing an exoskeleton as well as analyzing the evolution of inter-joint coordination during the exposition phase. This is a major challenge to address in order to enable widespread and safe use of exoskeletons in the future.

REFERENCES

[1] Y. Xu, V. Crocher, J. Fong, Y. Tan, and D. Oetomo, "Inducing Human Motor Adaptation without Explicit Error Feedback: A Motor Cost Approach," *IEEE Trans. Neural Syst. Rehabil. Eng.*, vol. 29, pp. 1403–1412, 2021.

[2] S. Iranzo, A. Piedrabuena, F. García-Torres, J. L. Martinez-De-juan, G. Prats-Boluda, M. Sanchis, and J. M. Belda-Lois, "Assessment of a Passive Lumbar Exoskeleton in Material Manual Handling Tasks under Laboratory Conditions," *Sensors*, vol. 22, no. 11, pp. 1–29, 2022.

[3] E. Rayssiguie and M. S. Erden, "A Review of Exoskeletons Considering Nurses," *Sensors*, vol. 22, no. 18, 2022.

[4] R. Shadmehr and F. A. Mussa-ivaldi, "Adaptive Task of Dynamics during Learning of a Motor Task," *J. Neurosci.*, vol. 14, no. 5, pp. 3208–3224, 1994.

[5] M. Mistry, P. Mohajerian, and S. Schaal, "Arm movement experiments with joint space force fields using an exoskeleton robot," *Proc. 2005 IEEE 9th Int. Conf. Rehabil. Robot.*, vol. 2005, no. May 2014, pp. 408–413, 2005.

[6] T. Proietti, E. Guigon, A. Roby-Brami, and N. Jarrassé, "Modifying upper-limb inter-joint coordination in healthy subjects by training with a robotic exoskeleton," *J. Neuroeng. Rehabil.*, vol. 14, no. 1, 2017.

[7] C. Latella, Y. Tirupachuri, L. Tagliapietra, L. Rapetti, B. Schirrmeister, J. Bornmann, D. Gorjan, J. Čamernik, P. Maurice, L. Fritzsche, C. Latella, Y. Tirupachuri, L. Tagliapietra, L. Rapetti, B. Schirrmeister, C. Latella, Y. Tirupachuri, L. Tagliapietra, L. Rapetti, J. Camernik, F. Nori, and D. Pucci, "Analysis of Human Whole-body Joint Torques during Overhead Work with a Passive Exoskeleton To cite this version : HAL Id : hal-03428469 Analysis of Human Whole-body Joint Torques during Overhead Work with a Passive Exoskeleton," 2021.

[8] T. Krasovsky and M. F. Levin, "Toward a better understanding of coordination in healthy and poststroke gait," *Neurorehabil. Neural Repair*, vol. 24, no. 3, pp. 213–224, 2010.

[9] Y. Tomita, M. R. Rodrigues, and M. F. Levin, "Upper Limb Coordination in Individuals With Stroke: Poorly Defined and Poorly Quantified," *Neurorehabil. Neural Repair*, vol. 31, no. 10-11, pp. 885–897, 2017.

[10] C. Shirota, J. Jansa, J. Diaz, S. Balasubramanian, S. Mazzoleni, N. A. Borghese, and A. Melendez-Calderon, "On the assessment of coordination between upper extremities: Towards a common language between rehabilitation engineers, clinicians and neuroscientists," *J. Neuroeng. Rehabil.*, vol. 13, no. 1, pp. 1–14, 2016. [Online]. Available: http://dx.doi.org/10.1186/s12984-016-0186-x

[11] P. Maurice, S. Ivaldi, J. Babič, J. Camernik, D. Gorjan, B. Schirrmeister, J. Bornmann, L. Tagliapietra, C. Latella, D. Pucci, and L. Fritzsche, "Objective and Subjective Effects of a Passive Exoskeleton on Overhead Work," *IEEE Trans. Neural Syst. Rehabil. Eng.*, vol. 28, no. 1, pp. 152–164, 2020.

[12] P. Garrec, Y. Friconneau, Y. Méasson, Y. Perrot, P. Garrec, Y. Friconneau, Y. Méasson, Y. P. Able, and T. Exoskeleton, "ABLE , an Innovative Transparent Exoskeleton for the To cite this version : HAL Id : cea-01588401 ABLE , an Innovative Transparent Exoskeleton for the Upper-Limb," *Int. Conf. Intell. Robot. Syst. INRIA*, 2008.

[13] N. Jarrassé, M. Tagliabue, J. V. Robertson, A. Maiza, V. Crocher, A. Roby-Brami, and G. Morel, "A methodology to quantify alterations in human upper limb movement during co-manipulation with an exoskeleton," *IEEE Trans. Neural Syst. Rehabil. Eng.*, vol. 18, no. 4, pp. 389–397, 2010.

[14] R. C. Oldfield, "The assessment and analysis of handedness: The Edinburgh inventory," *Neuropsychologia*, vol. 9, no. 1, pp. 97–113, 1971.

[15] J. F. O. Brien and J. K. Hodgins, "Automatic Joint Parameter Estimation from Magnetic Motion Capture Data," no. February 2015, pp. 1–8, 2000.

[16] K. Pearson, "On lines and planes of closest fit to systems of points in space," *London, Edinburgh, Dublin Philos. Mag. J. Sci.*, vol. 2, no. 11, pp. 559–572, 1901.

[17] J. Savin, C. Gaudez, M. A. Gilles, V. Padois, and P. Bidaud, "Evidence of movement variability patterns during a repetitive pointing task until exhaustion," *Appl. Ergon.*, vol. 96, no. May, p. 103464, 2021. [Online]. Available: https://doi.org/10.1016/j.apergo.2021.103464

[18] A. Forner-Cordero, O. Levin, Y. Li, and S. P. Swinnen, "Principal component analysis of complex multijoint coordinative movements," *Biol. Cybern.*, vol. 93, no. 1, pp. 63–78, 2005.

[19] M. C. Cirstea and M. F. Levin, "Improvement of arm movement patterns and endpoint control depends on type of feedback during practice in stroke survivors," *Neurorehabil. Neural Repair*, vol. 21, no. 5, pp. 398–411, 2007.

[20] A. K. Galgon and P. A. Shewokis, "Using mean absolute relative phase, deviation phase and point-estimation relative phase to measure postural coordination in a serial reaching task," *J. Sport. Sci. Med.*, vol. 15, no. 1, pp. 131–141, 2016.

[21] R. Burgess-Limerick, B. Abernethy, and R. J. Neal, "Relative phase quantifies interjoint coordination," *J. Biomech.*, vol. 26, no. 1, pp. 91–94, 1993.

[22] L. Seifert, H. Leblanc, R. Herault, J. Komar, C. Button, and D. Chollet, "Inter-individual variability in the upper-lower limb breaststroke coordination," *Hum. Mov. Sci.*, vol. 30, no. 3, pp. 550–565, 2011. [Online]. Available: http://dx.doi.org/10.1016/j.humov.2010.12.003

[23] K. Daunoravičienė, J. Žižienė, J. Pauk, A. Idzkowski, I. Raudonytė, A. Juocevičius, A. Linkel, and J. Griškevičius, "Stroke-affected upper extremity movement assessment via continuous relative phase analysis," *Meas. J. Int. Meas. Confed.*, vol. 110, pp. 84–89, 2017.

[24] N. Jarrassé, T. Proietti, V. Crocher, O. Robertson, A. Sahbani, G. Morel, and A. Roby-Brami, "Robotic exoskeletons: A perspective for the rehabilitation of arm coordination in stroke patients," *Front. Hum. Neurosci.*, vol. 8, no. DEC, 2014.

[25] J. Bessler-Etten, L. Schaake, G. B. Prange-Lasonder, and J. H. Buurke, "Assessing effects of exoskeleton misalignment on knee joint load during swing using an instrumented leg simulator," *J. Neuroeng. Rehabil.*, vol. 19, no. 1, pp. 1–18, 2022. [Online]. Available: https://doi.org/10.1186/s12984-022-00990-z

[26] J. C. Cowley and D. H. Gates, "Inter-joint coordination changes during and after muscle fatigue," *Hum. Mov. Sci.*, vol. 56, no. October, pp. 109–118, 2017.

[27] J. Savin, C. Gaudez, M. A. Gilles, V. Padois, and P. Bidaud, "Evidence of movement variability patterns during a repetitive pointing task until exhaustion," *Appl. Ergon.*, vol. 96, no. June, p. 103464, 2021. [Online]. Available: https://doi.org/10.1016/j.apergo.2021.103464

[28] C. Yang, S. Leitkam, and J. N. Coté, "Effects of different fatigue locations on upper body kinematics and inter-joint coordination in a repetitive pointing task," *PLoS One*, vol. 14, no. 12, pp. 1–14, 2019.